

Supporting information for

Sensing and Imaging of PPI *in vivo* using Lanthanide-based

Second Near-infrared Luminescent Probes

Yaoquan Su ^a, Lingyue Ye ^a, Jiayu Gu ^a, Lingzhi Zhao ^{*a}, Yunyun Zhou ^{*a} and
Juanjuan Peng ^{*a}

^a State Key Laboratory of Natural Medicine, the School of Basic Medical Sciences and Clinical Pharmacy, China Pharmaceutical University, Nanjing, Jiangsu 211198, China. Email: pjj@cpu.edu.cn; zhouyy@cpu.edu.cn; zlj@cpu.edu.cn

Contents

The characterizations of TA/Fe ³⁺ -DCNPs	S2-S7
The luminescence change of probe to PPI	S7-S13
The mechanisms study of the probe for PPI detection	S14-S16
PPI detection and safety study <i>in vivo</i>	S17

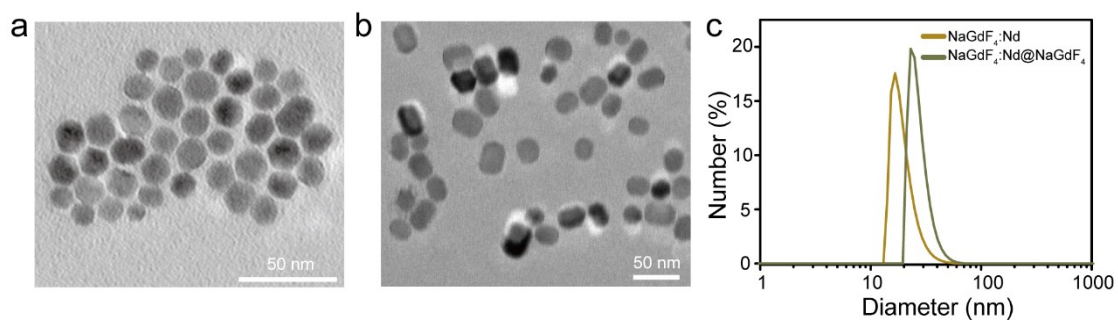


Fig. S1 The TEM images of (a) NaGdF₄:Nd and (b) NaGdF₄:Nd@NaGdF₄. (c) The size distribution of NaGdF₄:Nd and NaGdF₄:Nd@NaGdF₄ measured by the DLS method.

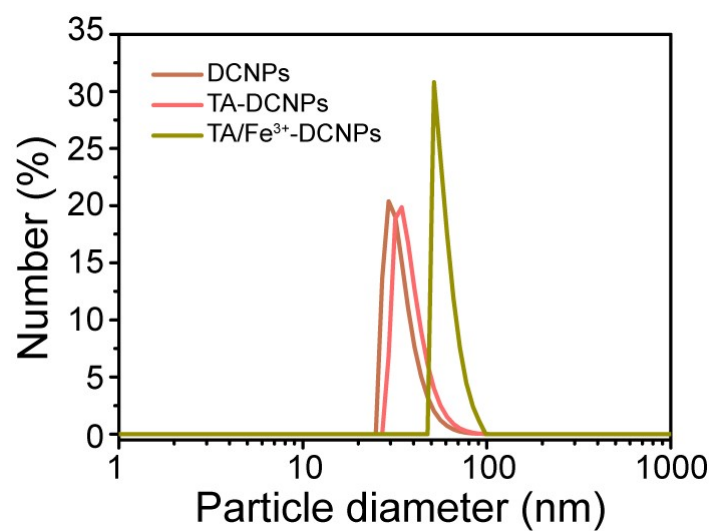


Fig. S2 Dynamic light scattering measurements of DCNPs, TA-DCNPs and TA/Fe³⁺-DCNPs.

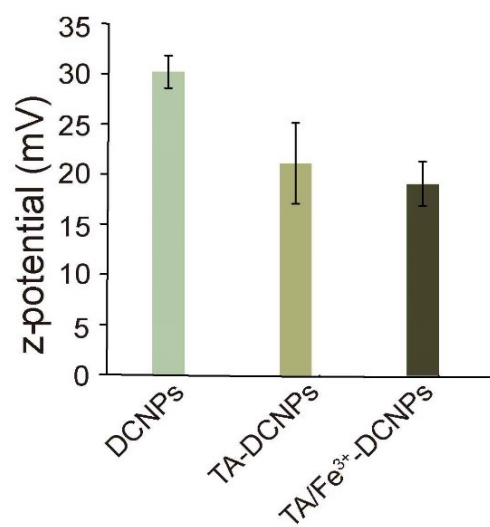


Fig. S3 The ξ -potentials of DCNP, TA-DCNPs, TA/ Fe³⁺-DCNPs.

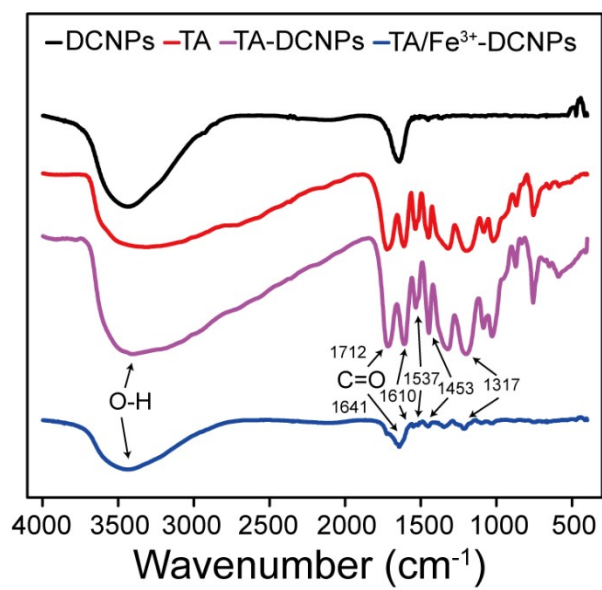


Fig. S4 The FT-IR spectra of DCNPs, TA, TA-DCNPs and TA/Fe³⁺-DCNPs.

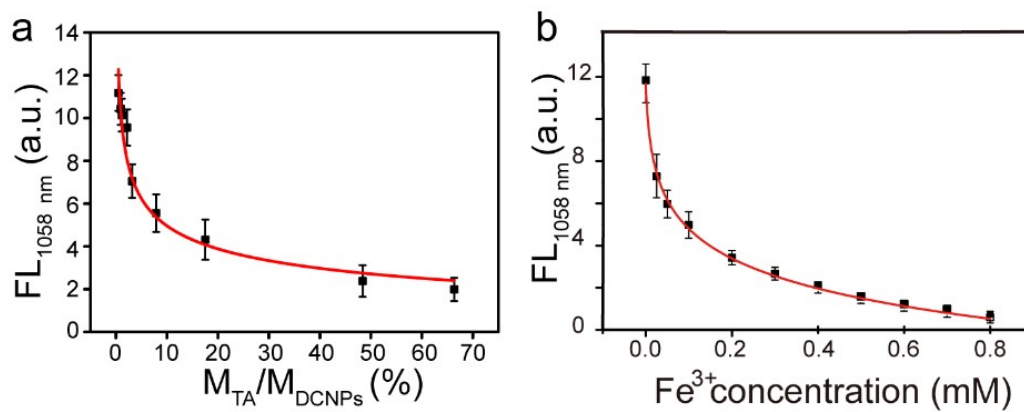


Fig. S5 (a) Plot of luminescence intensity at 1058 nm against the different mass ratio of TA:DCNPs (b) Plot of luminescence intensity at 1058 nm against the Fe^{3+} concentration ($n = 5$). The line joining the data points are the guide to the eye only.

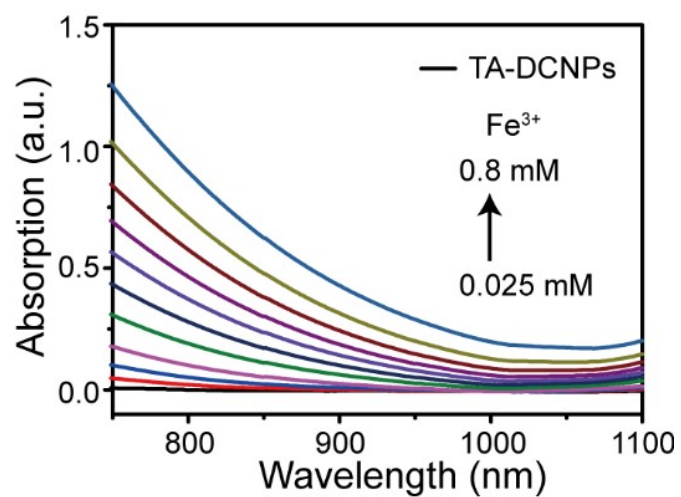


Fig. S6 The UV-vis spectra of TA-DCNPs at different concentration of Fe³⁺.

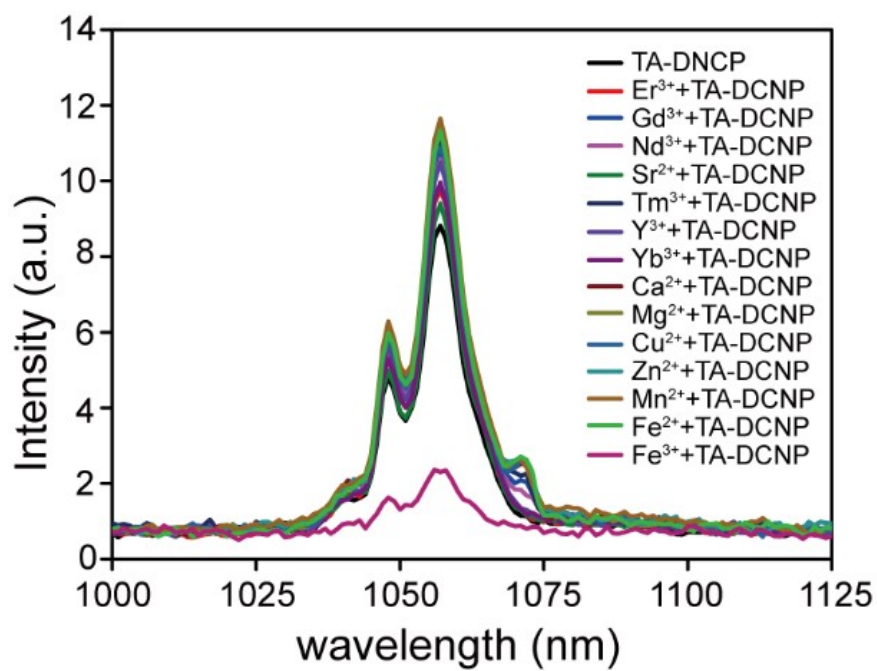


Fig. S7 The luminescence spectra of TA-DCNPs ($0.2 \text{ mg} \cdot \text{mL}^{-1}$) with different ions in PBS buffer (pH=7.2).

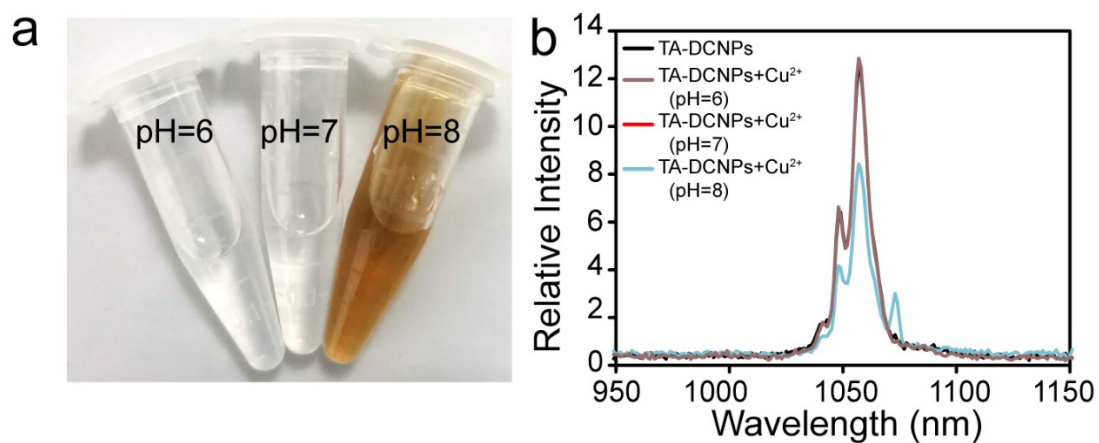


Fig. S8 The (a) pictures and (b) NIR-II spectra of TA-DCNPs+Cu²⁺ in PBS buffer with different pH values. The concentration of Cu²⁺ was 2 mM.

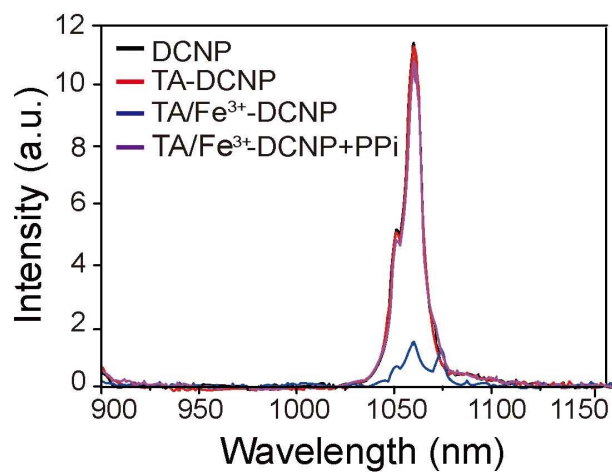


Fig. S9 The luminescence spectra of DCNPs, TA-DCNPs, TA/ Fe³⁺-DCNPs and TA/ Fe³⁺-DCNPs + PPI (2 mM). Excitation wavelength: 808 nm.

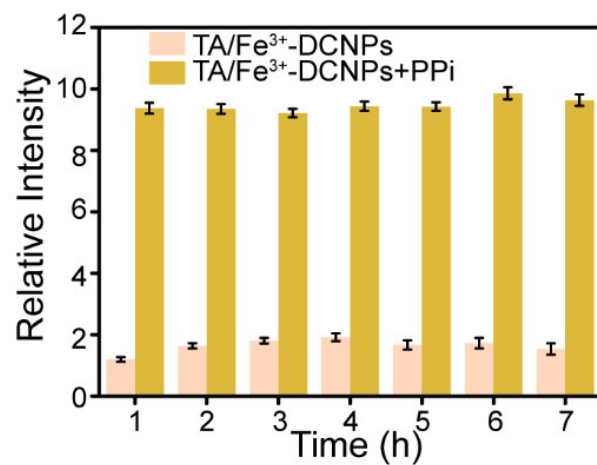


Fig. S10 The variation of the luminescence intensity of the TA/Fe³⁺-DCNPs and TA/Fe³⁺-DCNPs + PPI after 1-7 h.

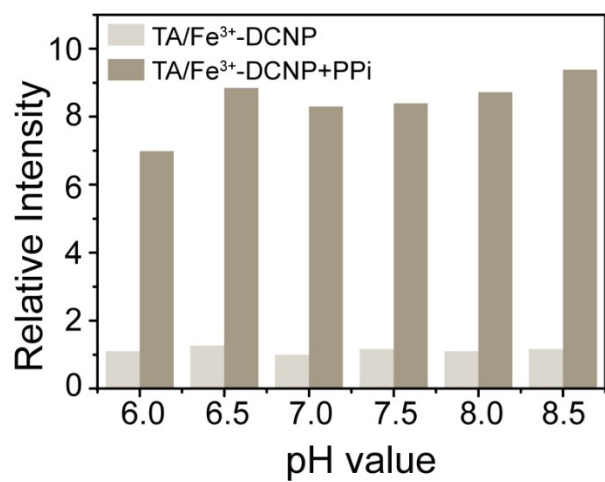


Fig. S11 The luminescence intensity of TA/Fe³⁺-DCNPs and luminescence TA/Fe³⁺-DCNPs response to PPi in different pH environments (HEPES).

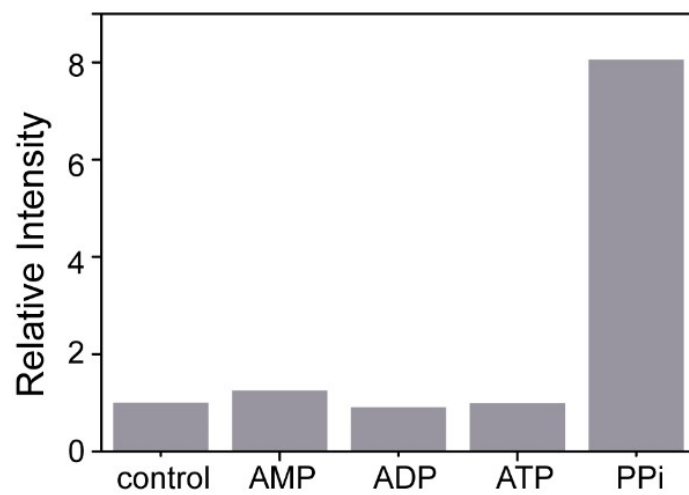


Fig. S12 The luminescence responses of TA/Fe³⁺-DCNPs (0.2 mg·mL⁻¹) in the presence of AMP, ADP and ATP (1 mM).

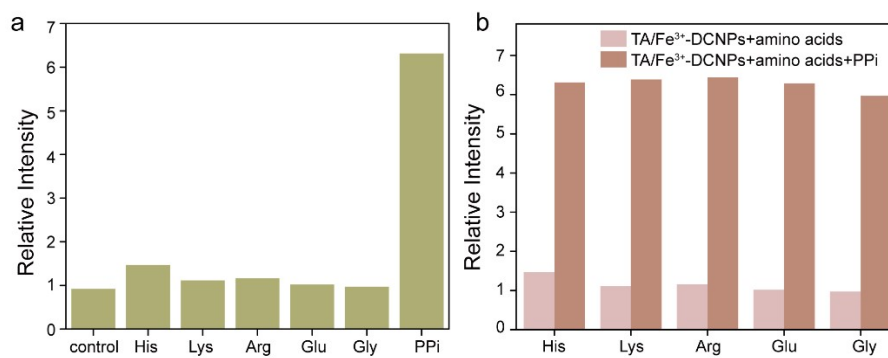


Fig. S13 (a) The luminescence responses of TA/Fe³⁺-DCNPs (0.2 mg·mL⁻¹) in the presence of several amino acids (1 mM). (b) The interference assay of the luminescence of TA/Fe³⁺-DCNPs with PPI in the presence of several amino acids.

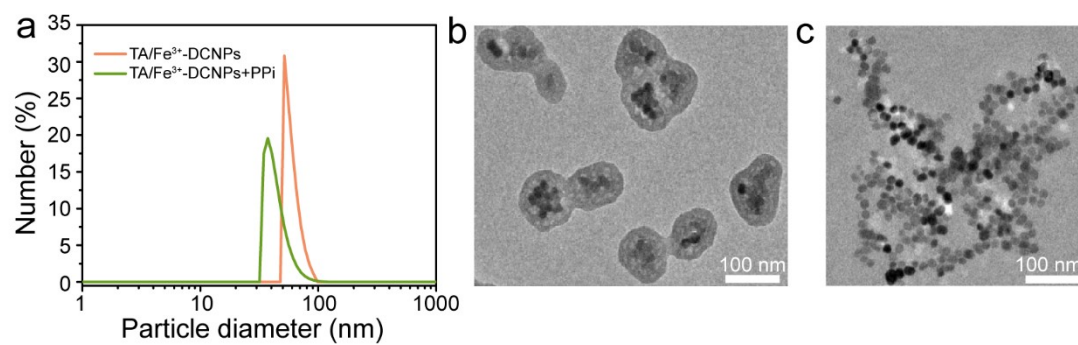


Fig. S14 (a) The DLS measurements of TA/ Fe³⁺-DCNPs and TA/Fe³⁺- DCNPs + PPi. The TEM images of TA/ Fe³⁺-DCNPs (b) and TA/Fe³⁺- DCNPs + PPi (c).

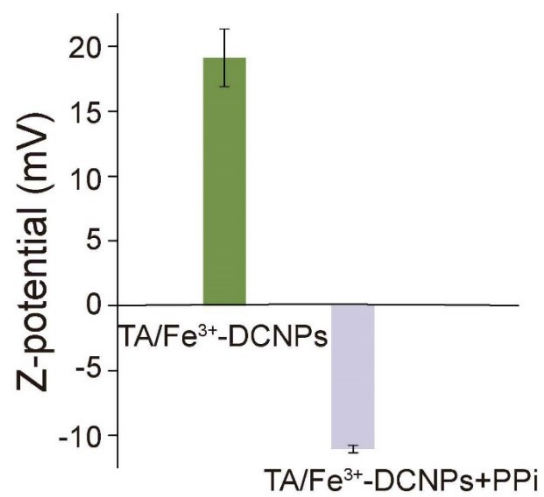


Fig. S15 Z-potential of TA/ Fe³⁺-DCNPs and TA/ Fe³⁺-DCNPs + PPi.

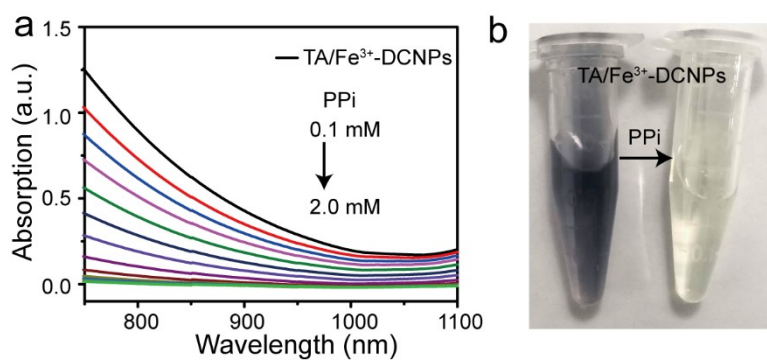


Fig. S16 (a) The UV-vis spectra of TA/ Fe³⁺-DCNPs at different concentration of PPI. (b) The photos of TA/ Fe³⁺-DCNPs before and after added PPI.

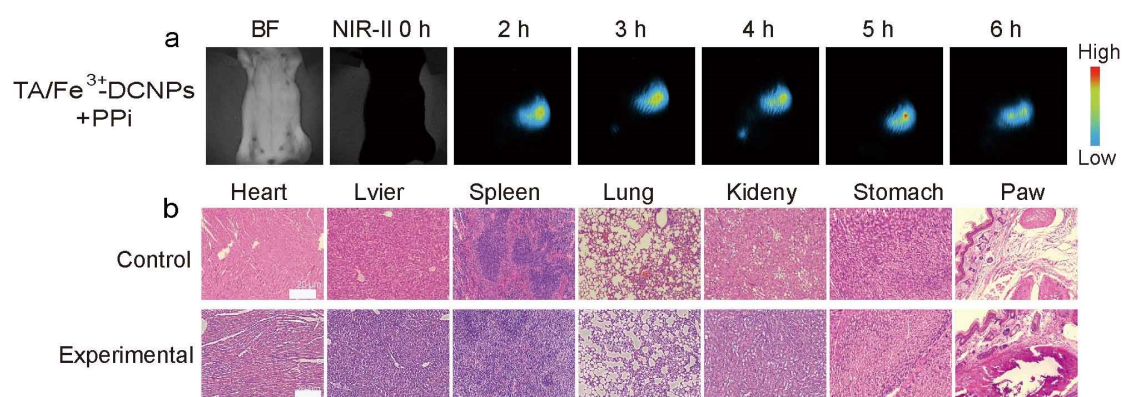


Fig. S17 (a) *In vivo* luminescence images of the mice at different times after gastric lavage of TA/ Fe³⁺-DCNPs and PPI. (b) H&E images of organs from mice treated with PBS or TA/Fe³⁺-DCNPs + PPI (0.25 mg·kg⁻¹), scale bars are 20 μm.